# Enhancement of US/CT registration applied to spinal surgery
Advanced Computer-Integrated Surgery (EN.601.656.01.SP18)

Eduardo A. Gonzalez (egonza31@jhmi.edu)
under the supervision of Professor Muyinatu A. Lediju Bell

## 1 Summary

Registration of multimodal images is a powerful tool for transferring preoperative plans into an intraoperative environment, thereby enhancing the surgeons accuracy to localize instruments in the operating room. Intraoperative ultrasound (US) to preoperative Computer Tomography (CT) registration is often a challenging task due to multiple factors, including the low signal-to-noise ratio of the US images and the presence of artifacts. This work explores Short Lag Spatial Coherence (SLSC) beamforming as an alternative to traditional Delay-And-Sum (DAS) ultrasound images to increase contrast and resolution for US-to-CT registration tasks. . The objective of this work is to explore Short-Lag Spatial Coherence (SLSC) beamforming as an alternative to delay-and-sum (DAS) beamforming to reduce speckle noise and enhance bone boundaries. In addition, we propose Locally Weighted SLSC (LW-SLSC) beamforming to further improve bone segmentation.

## 2 Introduction

In conventional surgery, there is a crucial need to accurately deliver preoperative information in an intraoperative situation. While existing technologies feature sophisticated system for needle tracking and surgical tool recognition, the physician still require to know if the overall operative region is correctly defined and located.

In medical imaging, Ultrasound (US) is an imaging modality that characterizes for using non-ionizing energy and with a relatively low cost in purchasing and maintenance in comparison with computer tomography (CT) and magnetic resonance imaging. Additionally, it is a suitable technique for intraoperative scanning of the human body due to the portable characteristic of the system (freehand probe in comparison with large systems that occupies the whole surgery room) and its simplicity to use (i.e. no extended training is required for a physitian to understand the imaging technique).

However, US is commonly affected with clutter artifacts and other reflections from tissues with high acoustic impedance. Therefore, compared to the other techniques, it usually feature low Signal-to-noise ration (SNR). For instance, in a region that is ideally anechoic (no reflections and therefore pitch black region), we can sometimes see brightness inside that region due to the reflections in the surrounding tisue. Moreover, in order to have good coupling with the surface (i.e. skin), physicians often apply a certain pressure along the normal axis of the tissue, which traduces in a certain degree of deformation. Hence, there isnt a rigid relationship between intraoperative information and preoperative information (i.e. CT)

In the past 10 years, there has been scarce investigation issuing US/CT registration. Between the most used approach, intensity-based registration has been used for registering US images with MRI applied in the brain, and US images with CT applied in the kidney. Other approaches rely on feature extraction (commonly edges recognition) with the use of sobel gradient and other techiques (see Fig. 1). Lastly, there has been few studies that explore the performance of the combination of the two aforementioned techinques, which are called multi-component similarity measurements.

## 3 Objective

The objective of the proposed project is to explore methods to improve accuracy of US-CT image registration through improved US image resolution. As specific aims there is:

- Enhance bony features in US images to improve resolution for automatic registration (**Done**)
- Develop a robust beamformer to improve the appearance of bone in US images (**Done**)
- Explore registration improvement when considering additional information from Photoacoustic (PA) images (**Done**)

# 4 Method

## 4.1 Setup

The overall initial framework is presented in Fig. 1. First, US channel is acquired and processed in offline mode with several beamforming techniques (DAS, SLSC and LW-SLSC). Then, in order to remove undesired reflection from water particles and bottom of the tank, segmentation using Fuzzy C-means was conducted. The algorithm divided each reconstructed US image in 3 regions: bone, water and not-image (due to the US transducer geometry) and selected the layer of bone only. Then, resampling was performed so the US image feature a similar pixel resolution than the CT data. Finally, registration was performed using Mattes Mutual information (fixed) as optimizer and least square method as metric.

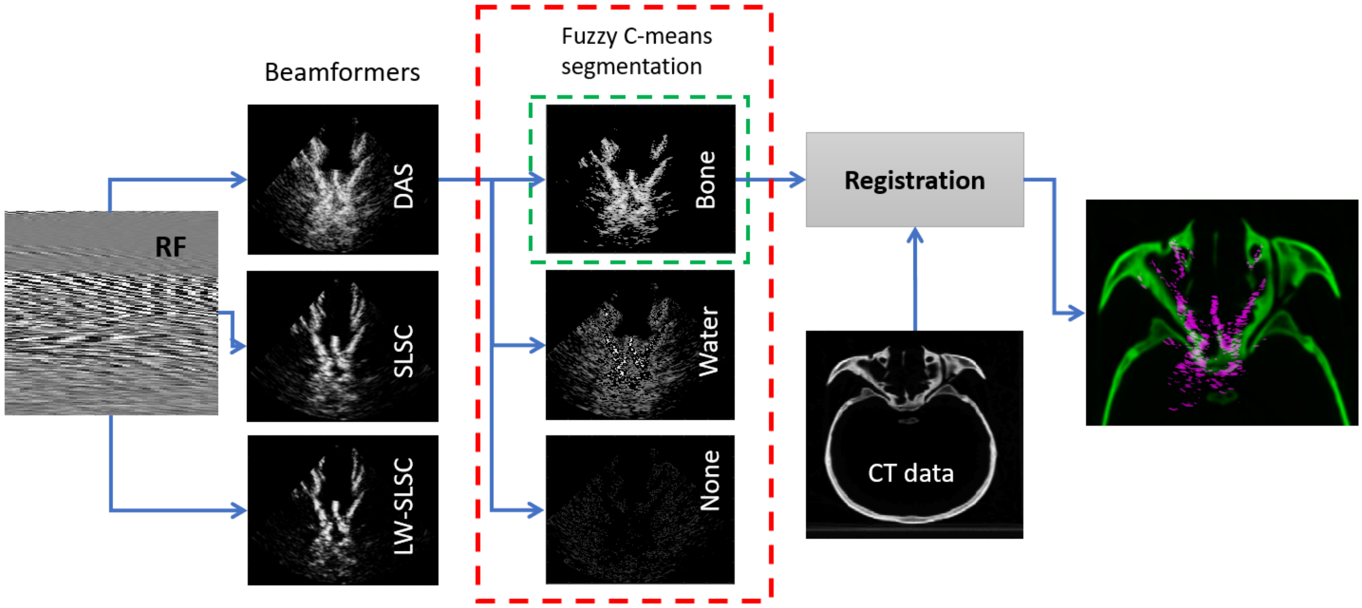


Figure 1: Initial scheme: RF is converted to several beamformed images that are later segmented for bone detection. Then, registration with CT is performed using a fixed Mattes Mutual information algorithm

Later, preliminary results of the framework in the human skull demonstrated that Fuzzy C-means segmentation did not benefit in the registration procedure. Furthermore, the improvement in the bone edges was already achieved with the SLSC and LW-SLSC implementation. Hence, the new framework removed the C-means segmentation step, as depicted in Fig. 2. This save us not only computational time but additional evaluation when changing the parameters in the Fuzzy C-means segmentation.

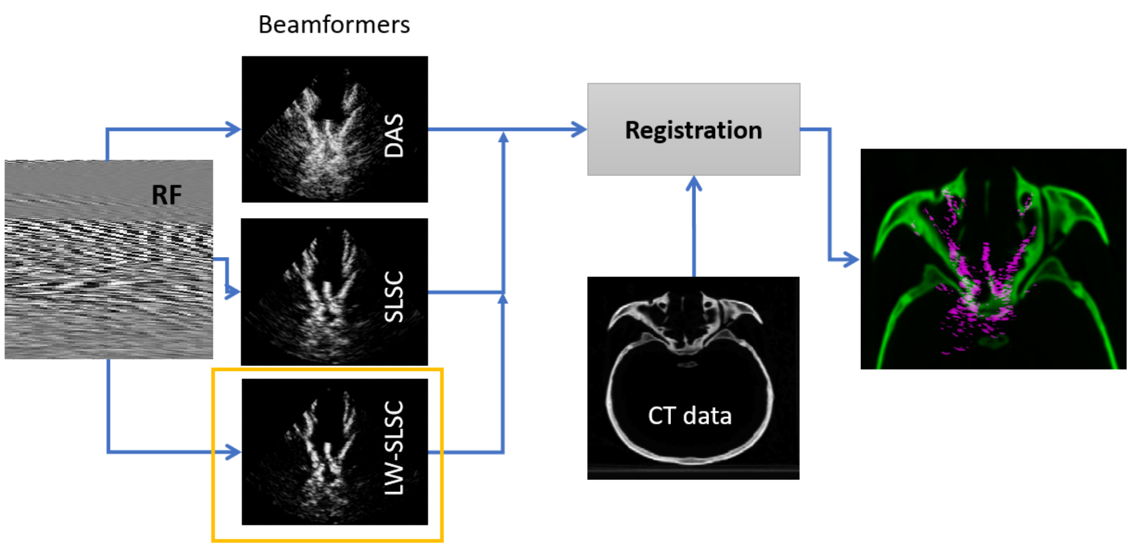


Figure 2: Upgraded scheme: Fuzzy C-means segmentation is removed since it does not contribute to the enhancement of the registration

## 4.2 US data beamforming

US channel data in freehand mode was acquired for 10 different views of a human vertebra submerged in deionized water using an Alpinion ECUBE-12R system and a SP1-5 phased array probe, with 3.8 MHz center frequency, 65 mm depth, 50 mm focus. The line density was set to the 192 in order to maximize the potential of SLSC and the novel proposed technique (LW-SLSC). Due to the nature of the acquisition, only 1 frame per view was processed, avoiding average over a number of frames that could reduce the resolution and contrast (since the probe was not in a fixed position).

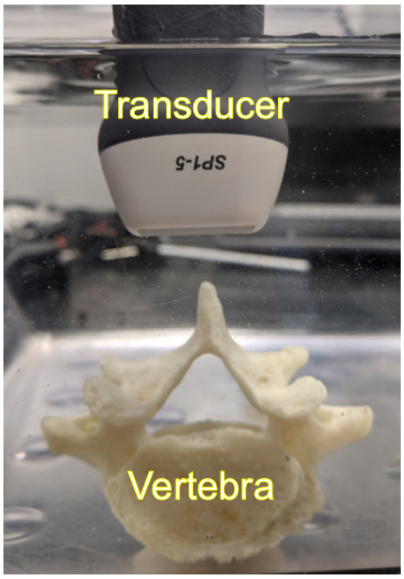


**DAS**

$$\tau(x_1, x, z) = \left(z + \sqrt{z^2 + (x - x_1)^2}\right)/c,$$

$$s(x, z) = \int_{x-a}^{x+a} RF\left(x_1, \tau(x_1, x, z)\right) dx_1.$$

**SLSC**

$$\hat{R}(m) = \frac{1}{N-m} \sum_{i=1}^{N-m} \frac{\sum_{n=n_1}^{n_2} s_i(n) s_{i+m}(n)}{\sqrt{\sum_{n=n_1}^{n_2} s_i^2(n) \sum_{n=n_1}^{n_2} s_{i+m}^2(n)}}$$

$$R_{\mathrm{sl}} = \int_1^M \hat{R}(m) \mathrm{d}m \approx \sum_{m=1}^{M} \hat{R}(m).$$

Figure 3: Left: US setup for acquisition. Top right: Algorithm for DAS. Bottom right: Algorithm for SLSC

The images were constructed several times when varying the reconstruction coefficient of each beamforming technique. SLSC images were computed with M varying from 1 to 50, and DAS images were created with the dynamic range (DR) varying from -60 to -20 dB. Later, we found that a significative difference was achieved in M=[1 25] for SLSC and DR=[-60 -40].

## 4.3 Locally Weighted Short Lag Spatial Coherence

Additionally, further enhancement of the bone edges can be achieved by implementing a regularized version of the coherence beamforming. Instead of averaging the cumulative sum up to a lag value M (out of a preselected total of N lags, where MN), LW-SLSC beamforming computes the weighted coefficients for N lags by minimizing the total variation of the weighted sum within a moving kernel. In order to preserve the high resolution located at higher lags, this adaptive solution is regularized using the L2-norm with a gradient operator.

$$\hat{w_i} = \mathrm{argmin}\{\|\mathrm{TV}(w_i K_i)\|^2 + \alpha \|\nabla w_i\|^2\}$$

Figure 4: LW-SLSC: Total variation is being computed in the cost function. The objective is to find the optimum w values that varies along each small kernel K A regularization term using a gradient operator is added to preserve high resolution commonly found at larger lags

The factors that contribute to the quality of the LW-SLSC are mainly the distribution of the kernels (OL=overlap), the size of the kernel, and the regularization term $\alpha$. In this project, we have adjusted the size and overlap of the kernel in a way that can improve the edges and the uniformity of the bone without consuming excessive computational time. Hence, the windows was set to 1.20 mm (lateral) x 1.92 mm (axial) and a 50% overlap. Likewise, to optimize the w values with information of high resolution, all LW-SLSC were processed up to 50 lags. For the regularization coefficient, a conventional L-curve method was applied over a set of vertebra results to find the optimized value. In this case, the value was 0.1.

## 4.4 Finding and evaluating a good similarity metric

Initially, the idea of evaluating the registration performance was through CT markers already located in a custom vertebra samples and perform intensity based comparison between the overlapped points in US/CT. However, the dots didn't completely showed in the US reconstruction, mainly because the markers are designed for high contrast in CT only, and have not been evaluated for US before. Hence, an adequate metric was required to quantitatively assess the registration performance when using DAS/SLSC/LW-SLSC.

Consider a set of reconstructed images of the human vertebra, as showed in Fig. 4. Qualitatively speaking, there is a significant improvement in the similarity of US images when using SLSC and LW-SLSC in comparison with conventional DAS. Hence, the metric chosen must reflect this trend when comparing the overlaped US/CT. It is worth mentioning that all DAS/SLSC/LW-SLSC sucessfully followed the tilted vertebra and thus, they are all well registered.

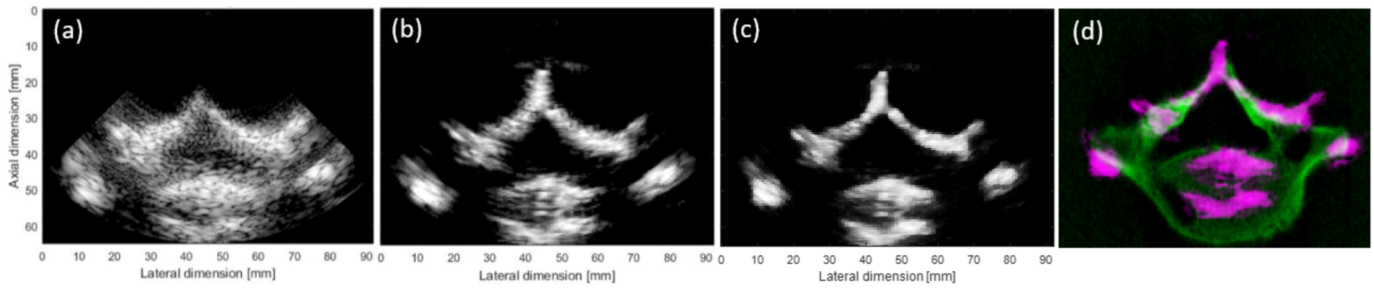


Figure 5: Reconstructed US with: (a) DAS, (b) SLSC, (c) LW-SLSC. (d) Registered CT/LW-SLSC

A set of metrics was evaluated for similarity quantification, which were proposed and previously used in the literature. Mainly, the Pixel Intensity Uniformity (PIU), Mutual Information, Entropy difference, Normalized Cross Correlation (NCC) and Gradient Correlation (GC) were tested.

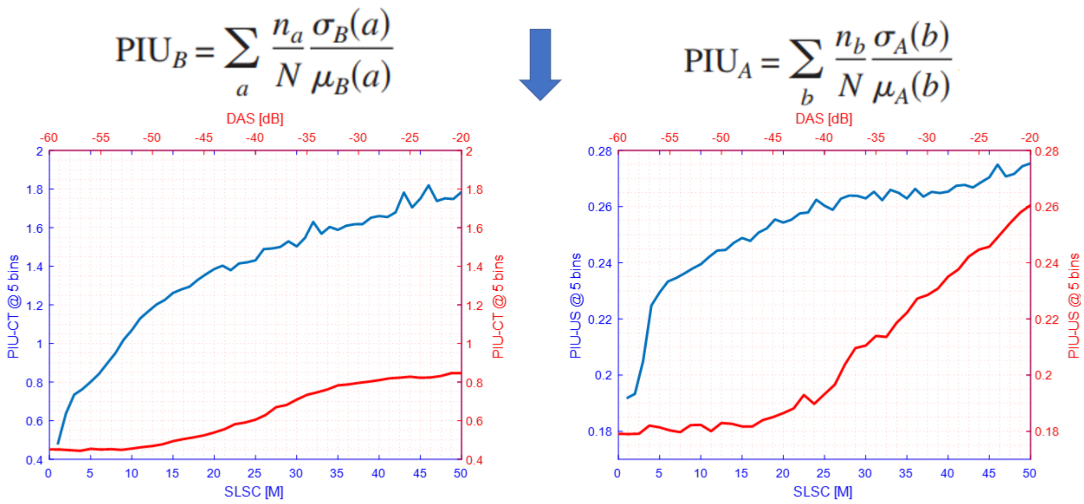


Figure 6: Pixel Intensity Uniformity (PIU) metric for CT/US (left) and US/CT (right). The lower, the better

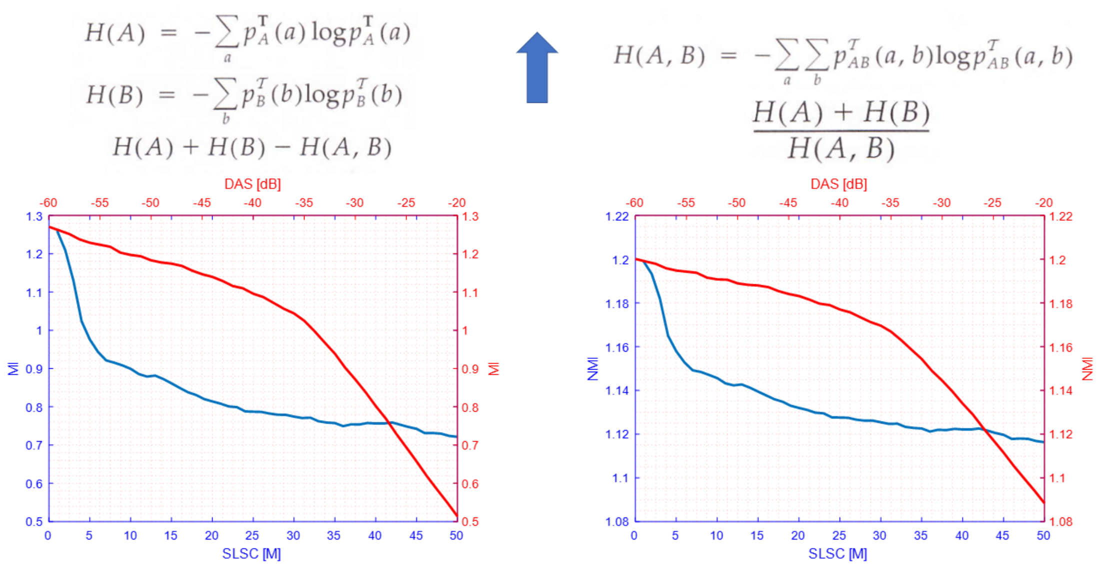


Figure 7: Mutual information (left) and Entropy difference (right) metric. The higher, the better

$$\mathrm{NCC} = \frac{\sum_{(i,j)\in\Omega^T}[A(i,j)-\bar{A}][B^T(i,j)-\bar{B}]}{\sqrt{\sum_{(i,j)\in\Omega^T}[A(i,j)-\bar{A}]^2\sum_{(i,j)\in\Omega^T}[B^T(i,j)-\bar{B}]^2}}.$$

$$0.5[\mathrm{NCC}(\frac{\partial A(i,j)}{\partial i},\frac{\partial B(i,j)}{\partial i})+\mathrm{NCC}(\frac{\partial A(i,j)}{\partial j},\frac{\partial B(i,j)}{\partial j})]$$

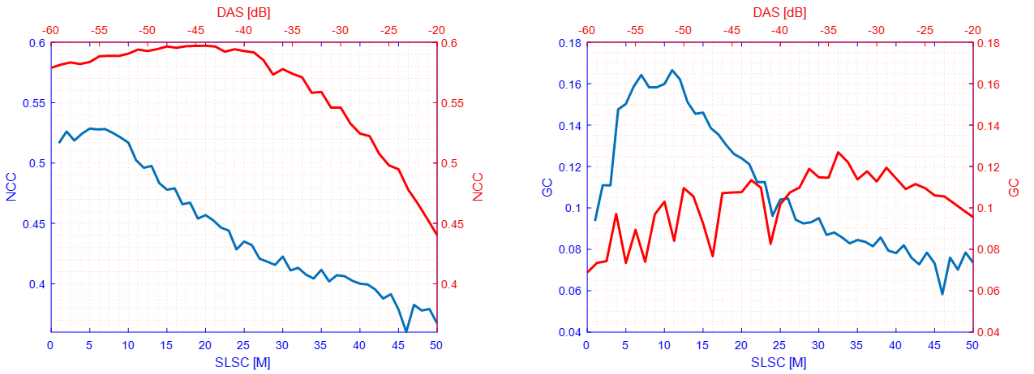


Figure 8: Normalized cross correlation (left) and gradient correlation (right). The higher, the better

As observed, the first 5 metrics fail to properly represent the similarities of SLSC/CT compared to DAS/CT. This is mainly because they are intensity based similarity and, while is true that SLSC has better edges, it has lower pixel density. Hence, the Gradient Correlation (GC) was measured to evaluate the bone structure similarity of each ultrasound imaging method when compared to CT images.

# 5 Results

Example CT, DAS, SLSC and LW-SLSC images are shown in Fig. 1 alongside the mean  standard deviation of GC measurements. Overall, SLSC outperforms DAS for a range of parameters commonly used in the literature (e.g., M=5-25, DR=-50 to -60 dB) when considering the similarity of bone structures in the CT and US-based images. An additional improvement is observed with LW-SLSC over SLSC (e.g., 8.2 dB mean contrast-to-noise ratio increase, 0.10 mean GC increase).

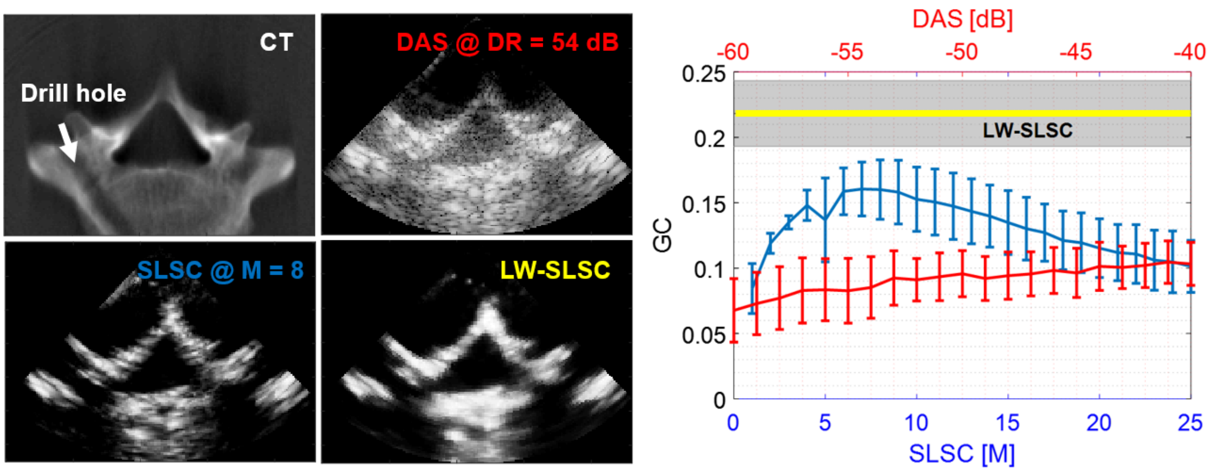


Figure 9: Left: examples of reconstructed CT, DAS, SLSC and LW-SLSC images. Observe that both SLSC and LW-SLSC have similar lateral resolution. Right: Mean  standard deviation of GC measurements when comparing DAS, SLSC and LW-SLSC images to CT images. Note that the neither x-axis applies to the LW-SLSC result as the multiple possible parameters were fixed for all 10 images

In order to assess the level of accuracy that the GC factor provides regarding registration and similarity, intensional misalignment (performed manually) of the reconstructed US and CT images was performed from 30 to -30 degrees and then overlapped. Note that no registration step was conducted. From the results, an empirical threshold vs the parameter for DAS and SLSC can be generated around 5 degrees of rotation, which corresponds to GC values less than 0.06.

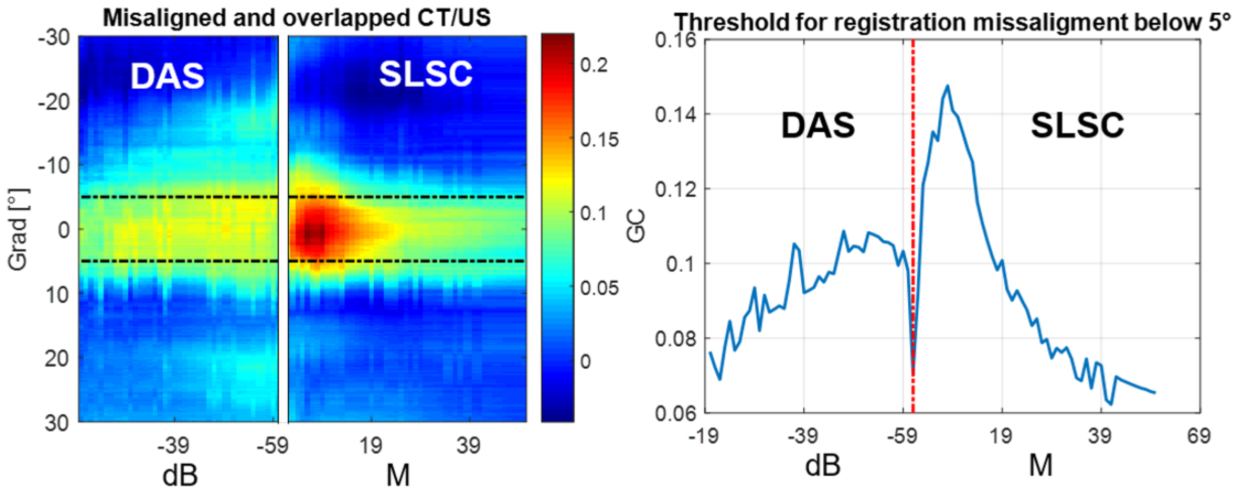


Figure 10: Intentional misalignment, shows poor performance beyond ± 5 degree rotation

Later, registration of a set of images was conducted when the CT was rotated a certain angle (in the same range of the previous experiment). The empirical threshold previously calculated was in accordance with registration results. Fig. 11 shows the GC estimation for registered DAS and SLSC images, as well as example of poor registration.

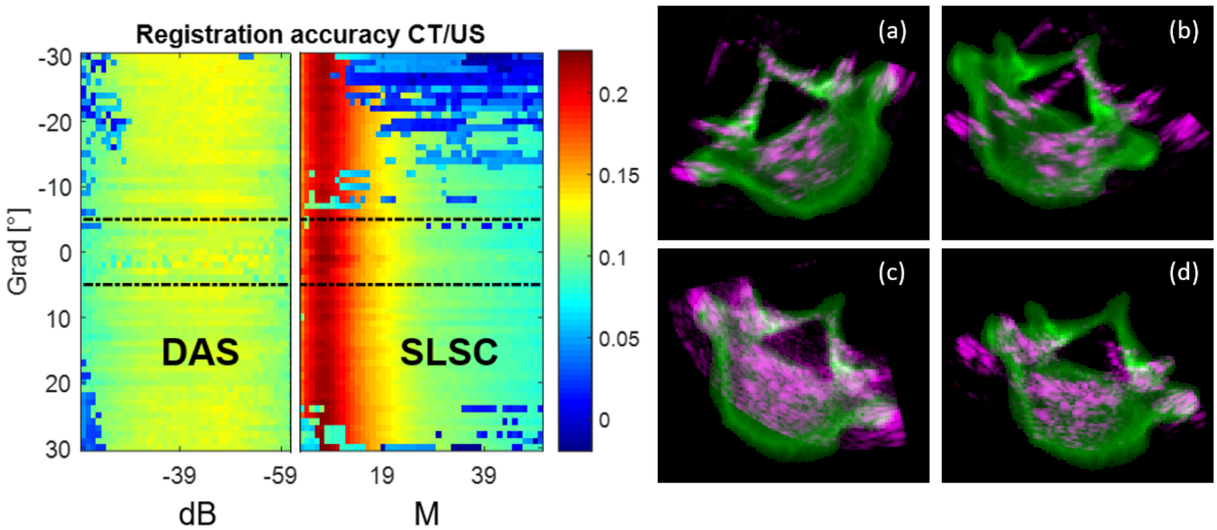


Figure 11: Left: Registration results around ± 30 degrees. (a) Well registered SLSC at -26°, (b) Poor registered SLSC at +26°, (c) Poor registered DAS at +30°, (d) Poor registered DAS at -20°

Finally, the same experiment was conducted with the addition of Photo acoustic (PA) signals. We used a caterer operating at 750 wavelength and 70% energy firing to the drill hole cavity inside the vertebra (see Fig. 9). Then, channel data as for both ultrasound and photo acoustic was acquired. The additional data from PA can be considered as a separate image that is already registered to the US images. Then, applying an advanced beamforming (either SLSC or LW-SLSC) and registering to the CT image, is it possible to track the location of the PA signal. In practice a PA signal can be installed to the tip of an operating tool, which could be tracked inside the human vertebra. However, this is a preliminary result, and more experiments are required for such statement.

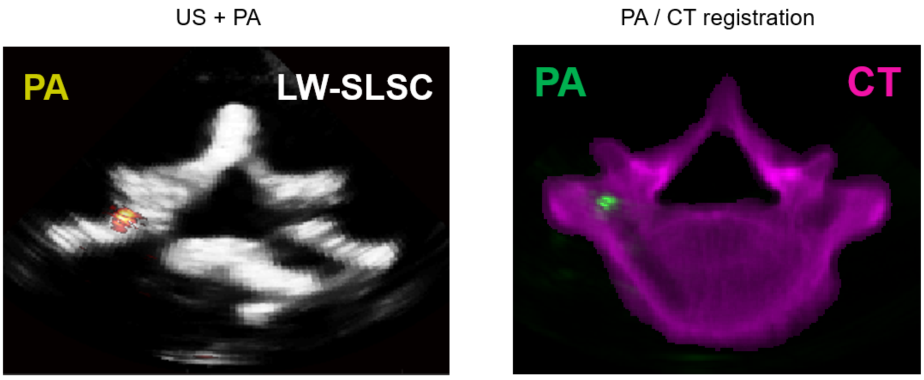


Figure 12: Preliminary resulst of PA/CT registration

## 6 Conclusion

In this study, a first time implementation of advanced beamforming techniques was applied for segmenting the bone structure of human vertebra. Initial results suggest that SLSC and LW-SLSC provide improved bone segmentation over DAS, with possible applications to improving US-CT registration for spine surgery. Likewise, the chose metric provides information not only for registration performance but for similarity of the bone shape between US and CT images. On the other hand, preliminary results of photoacoustic(PA)-CT registration could aid in tracking of surgical tools inside the human vertebra.

## 7 Future Work

The next step is to evaluate the current implementation with volumetric US/CT data, as the structure complexity could hinder or further differentiate the registration performance between US images. On the other hand, experiments on ex-vivo human spine with soft tissue and/or in-vivo samples is necessary to evaluate the effects of additional scatter and clutter that is commonly present in real data.

## 8 Publications

Eduardo A. Gonzalez, Muyinatu A. Lediju Bell, *Segmenting bone structures in ultrasound images with Locally Weighted SLSC beamforming*, IUS 2018 (in review)

## 9 Acknowledgments

Thank you to Michelle Graham for assisting me with the acquisition of CT / PA data

## 10 Bibliography

- Roche et al. Rigid Registration of 3-D Ultrasound With MR Images: A New Approach Combining Intensity and Gradient Information, 2001.
- Wein et al. Simulation and Fully Automatic Multimodal Registration of Medical Ultrasound, 2007.
- Wein et al. Automatic CT-ultrasound registration for diagnostic imaging and image-guided intervention, 2008.
- Bell et al. Short-Lag Spatial Coherence of Backscattered Echoes: Imaging Characteristics, 2011.
- Wong et al. Real-time ultrasound-guided spinal anesthesia using the SonixGPS needle tracking system: a case report, 2013.
- Shubert et al. A novel drill design for photoacoustic guided surgeries, 2017